Journal of Engineering, Technology & Applied Science
p-ISSN: 2721-7949, e-ISSN: 2721-8090

Original Research Paper

Fuzzy-PID Control Design and Performance Analysis for PMSM Drives in Electric Vehicles

Kalyankolo Umaru[1*], Nafuna Ritah[2], Mugabe Rodney[3], Yudaya Nansukusa[2], Salaama Asikuru[1], Noah Ochima[1], Pison Mutaburura[1], Kalyankolo Zaina[4]

[1] *Department of Electrical Engineering and Automation, Muni University. Arua, Uganda.*
[2] *Department of Computer and Information Science, Muni University. Arua, Uganda.*
[3] *Department of Electrical and Control Engineering, International University of East Africa (IUEA). Kampala, Uganda.*
[4] *Department of Information Technology, Faculty of Computing and Informatics, Mbarara University of Science and Technology. Mbarara, Uganda.*

Article History
Received:
07.08.2025

Revised:
26.08.2025

Accepted:
03.09.2025

***Corresponding Author:**
Kalyankolo Umaru
Email:
u.kalyankolo@muni.ac.ug

Abstract: The increasing demand for high performance and energy efficient electric vehicles has driven research into advanced motor control strategies for Permanent Magnet Synchronous Motors. This study investigates the design and performance evaluation of a Fuzzy PID controller as the speed regulator to address the limitations of the typical PID controllers in EV propulsion and a field-oriented control strategy is used. A conventional PID controller is initially implemented and tuned using the Ziegler-Nichols closed loop method. A Fuzzy Inference System is developed and then integrated with the PID controller to form a hybrid Fuzzy PID controller capable of adjusting the PID gains in real time. The performance of both controllers is evaluated under various test scenarios including speed variations, load disturbances, and parameter changes. Simulation results demonstrate that the Fuzzy PID controller significantly reduced overshoot by 0.5%, reduced rise time by 32.04%, improved settling time by 8.04%, and therefore enhanced system stability and responsiveness compared to the typical PID controller. These improvements validate the effectiveness of fuzzy logic in managing the uncertainties associated with PMSM control in EV applications.

Keywords: FOC, Fuzzy Logic, MATLAB, PID Controller, PMSM.

Journal of Engineering, Technology & Applied Science, vol. 7, no. 3, pp. 127-148, December 2025. **DOI: 10.36079/lamintang.jetas-0703.917**

1. Introduction

The advancement in electric vehicle (EV) technology has increased the demand for more efficient motor drives. Among various motor types, the Permanent Magnet Synchronous Motor (PMSM) has gained significant attention due to its superior performance. It is an AC synchronous motor where permanent magnets embedded in the rotor, generate a constant magnetic field, eliminating the need for external excitation. It has no rotor windings, which means minimal copper losses in the rotor and thus high efficiency. This motor provides high torque even at low speeds and its capable of high speeds without sacrificing torque. It is light and compact which is ideal for space constrained EV designs. It lacks brushes and commutators which reduces wear and maintenance needs [1] [2] [3] [4]. The Proportional-Integral-Derivative (PID) controller is a feedback controller that calculates an error value as the difference between a desired set point and a measured process variable. The controller then applies a correction based on proportional, integral, and derivative terms, represented by three constants (K_p, K_i and K_d), to minimize the error over time [5] [6] [7] [8]. Fuzzy logic is a mathematical method that deals with approximate reasoning rather than fixed and exact values. Fuzzy logic was invented by Lotfi A. Zadeh, a professor at the University of California, Berkeley. He introduced the concept in his seminal paper, "Fuzzy Sets," published in 1965 [9] [10] [11] [12].

PMSMs in EVs experience varying load conditions, changing speed and torque demands imposed by inclines or declines in the roads. Temperature variations may affect stator resistance and magnet strength altering motor performance, extreme temperatures or over current scenarios may also degrade the permanent magnets [6] [7]. Traditional PID controllers are parameter sensitive, that is to say variations in motor parameters (stator resistance, inductance) due to temperature changes during extended operation can degrade PID performance. PID controllers also struggle to reject load disturbances efficiently. The PID tuning process is often trial and error or relies on methods like Ziegler-Nichols, Cohen-Coon which provide suboptimal performance under varying system dynamics [5] [13] [14] [15]. Advanced methods such as Model Predictive Control (MPC) and Sliding Mode Control (SMC) offer improved robustness and transient performance, but their high computational cost and issues such as chattering restrict practical real time deployment on embedded EV hardware. Direct Torque Control (DTC), although fast and simple, suffers from high torque and flux ripple and variable switching frequency, making it unsuitable for smooth, energy efficient EV operation [7] [8] [16] [17].

This calls for robust control strategies that can maintain consistent performance across diverse operating conditions. Fuzzy-PID control offers a promising alternative by eliminating strict reliance on mathematical models and instead using rule-based reasoning that accommodates nonlinearities and parameter variations. Its adaptive rule structure enables real-time adjustment of control actions, reducing torque ripple, improving energy efficiency, and lowering computational requirements compared to MPC and SMC. This makes fuzzy-based control strategies more practical for embedded EV drive systems and readily scalable to other AC machine types [7] [9] [10] [16]. Prior studies have not adequately addressed the combined effects of nonlinear PMSM parameter variations, external disturbances such as sensor noise, actuator limitations, and temperature deviations in real world EV conditions. Existing fuzzy-PID approaches typically tune only the controller output rather than independently adjusting each PID gain, limiting adaptability and control precision [18] [19]. This paper offers independent tuning of each leg of the PID controller based on real time motor behavior for more adaptive control, accounting for external disturbances by using noise filters and investigating the effects of temperature variations on the control strategy.

The objectives of this research are to design a mathematical model of a Permanent Magnet Synchronous Motor (PMSM) that accurately represents its steady-state and dynamic characteristics, and to integrate this model with a PID controller to evaluate its performance under various operating conditions. Furthermore, the study aims to optimize the PID control parameters using a Fuzzy Inference System to enable adaptive control and achieve improved performance. Finally, the performance of the Fuzzy PID controller will be compared with that of the conventional PID controller by analyzing their speed response plots, focusing on key performance metrics such as settling time and overshoot.

2. Literature Review

2.1. The Permanent Magnet Synchronous Motor

A permanent magnet synchronous motor has two main parts; the stator which is the stationary part and the rotor, the rotating part. The stator consists of an outer cylindrical frame, a core which provides a path for the magnetic flux and stator windings as shown in Figure 1.

Journal of Engineering, Technology & Applied Science, vol. 7, no. 3, pp. 127-148, December 2025. **DOI: 10.36079/lamintang.jetas-0703.917**

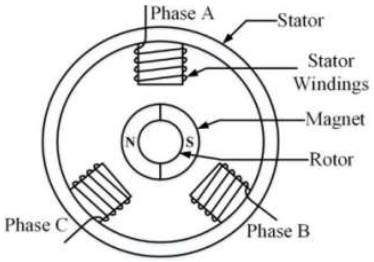

Figure 1. PMSM Structure [2]

The stator is similar to that of an induction motor, consisting of a laminated steel core with three phase windings, for a three phase PMSM. These windings are physically distributed 120º apart to produce a rotating magnetic field when energized [7] [20] [21]. The rotor contains permanent magnets instead of windings or squirrel cages. The magnets are embedded or surface mounted on the rotor core. The operation of a PMSM is based on the interaction between the rotating magnetic field produced by the stator windings and the static magnetic field of the rotor magnets [10] [22] [23]. When three phase AC currents are applied to the stator windings, they generate a rotating magnetic field. They create three-time varying magnetic fields that are spatially 120° apart [7] [16] [24] [25]. The superposition of these fields results in a single magnetic field that rotates continuously around the stator. This behavior is due to the nature of three phase AC systems and the sinusoidal variation of the currents. The direction of rotation is determined by the sequence of the three phase currents. The rotor, which contains permanent magnets, aligns itself with the rotating magnetic field, causing the rotor to rotate synchronously with the stator field. Torque is produced due to the magnetic attraction and repulsion between the stator and rotor fields. In IPMSMs, additional torque is generated through reluctance torque due to salience [26] [27]. The motor speed is controlled by varying the frequency of the stator currents, while the torque is controlled by adjusting the amplitude and phase of the currents.

2.2. Electrical Circuit of a PMSM

The stator windings are modelled as resistances and inductances in series with back emfs induced by the rotor magnets [8].

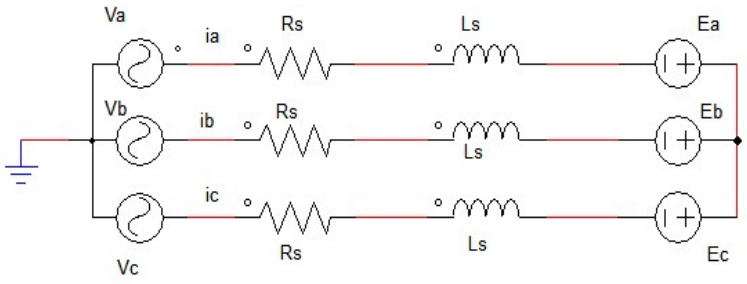

Figure 2. Electrical Circuit of a PMSM

2.3. PMSM Mathematical Modelling

The *dq* model is based on a transformation of the three-phase stationary reference frame into a rotating reference frame aligned with the rotor. The purpose is to simplify the analysis and control of PMSMs by converting the sinusoidal variables into DC like quantities in the rotor reference frame.

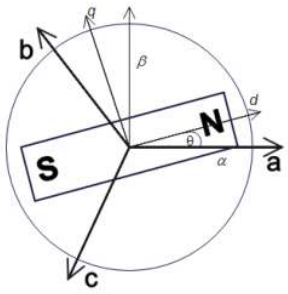

Figure 3. Reference Frames

1) ABC Frame

The voltage equations in the frame are given as:

$$\upsilon_a = Ri_a + \frac{d\lambda_a}{dt} \tag{1}$$

$$\upsilon_b = Ri_b + \frac{d\lambda_b}{dt} \tag{2}$$

$$\upsilon_c = Ri_c + \frac{d\lambda_c}{dt} \tag{3}$$

The flux linkages are related to the currents and rotor position by,

$$\lambda_a = L_s i_a + \lambda_m \cos\theta_r \tag{4}$$

$$\lambda_b = L_s i_b + \lambda_m \cos\left(\theta_r - \frac{2\pi}{3}\right) \tag{5}$$

$$\lambda_c = L_s i_c + \lambda_m \cos\left(\theta_r + \frac{2\pi}{3}\right) \tag{6}$$

The back emfs are sinusoidal and depend on the rotor position θ_r. The model is difficult to analyse because it involves sinusoidal time varying quantities. To simplify, we transform this system into the rotating reference frame.

2) Clarke's Transformation

The three phase *abc* frame is converted into a two phase αβ stationary frame. The αβ0 frame is orthogonal, with axes fixed in space [12]. For a balanced system the zero-sequence component is omitted as the matrix equation below shows, where f stands for electrical quantities; current or voltage.

$$\begin{bmatrix} f\alpha \\ f\beta \end{bmatrix} = \frac{2}{3}\begin{bmatrix} 1 & \frac{-1}{2} & \frac{-1}{2} \\ 0 & \frac{\sqrt{3}}{2} & \frac{-\sqrt{3}}{2} \end{bmatrix}\begin{bmatrix} fa \\ fb \\ fc \end{bmatrix} \tag{7}$$

The factor 2/3 ensures that the magnitude of the transformed vector remains consistent with the original three phase system.

3) Park's Transformation

The stationary αβ frame is transformed into the rotating dq0 reference frame aligned with the rotor. This transformation is time dependent and uses the rotor position. For a balanced system the zero-sequence component is ignored [12].

$$\begin{bmatrix} fd \\ fq \end{bmatrix} = \begin{bmatrix} \cos(\theta_r) & \sin(\theta_r) \\ -\sin(\theta_r) & \cos(\theta_r) \end{bmatrix}\begin{bmatrix} f\alpha \\ f\beta \end{bmatrix} \tag{8}$$

Journal of Engineering, Technology & Applied Science, vol. 7, no. 3, pp. 127-148, December 2025. **DOI: 10.36079/lamintang.jetas-0703.917**

4) DQ Frame Equations

In the *dq* frame, the voltage equations for a PMSM are:

$$v_d = Ri_d + \frac{d\lambda_d}{dt} - \omega_s \lambda_q \tag{9}$$

$$v_q = Ri_q + \frac{d\lambda_q}{dt} + \omega_s \lambda_d \tag{10}$$

where,

$$\lambda_d = \lambda_{ad} + \lambda_m = L_d i_d + \lambda_m \tag{11}$$

$$\lambda_q = \lambda_{aq} = L_q i_q \tag{12}$$

The cross-coupling terms $\omega L_d i_d$ and $\omega L_q i_q$ represent the interaction between the axes. $\omega \lambda_m$ represents the back emf from the permanent magnet flux [10]. The equivalent circuit of the PMSM as shown in Figure 4.

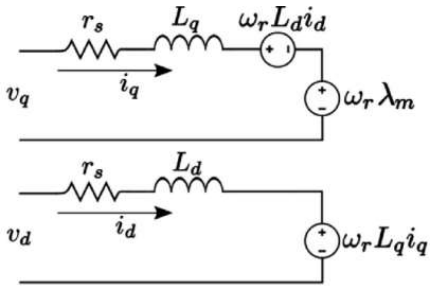

Figure 4. Equivalent Circuit *dq* Model [8]

Torque Equation

The electromagnetic torque, which is power divided by mechanical speed can be represented as:

$$T_e = \frac{3}{4} P[\lambda_m i_q + (L_d - L_q) i_d i_q] \tag{13}$$

For SPMSMs, $L_d = L_q$, so the torque equation simplifies to:

$$T_e = \frac{3}{4} P[\lambda_m i_q] \tag{14}$$

Mechanical dynamics of the rotor

$$J\frac{d\omega}{dt} + B\omega = T_e - T_L \tag{15}$$

2.4. PID Tuning

The process of adjusting the k_p, k_i, and k_d of a PID controller to achieve a fast response time, minimal overshoot, accurate setpoint tracking, and stable system performance. Figure 5, shows a PID controller connected to a plant.

$$u(t) = k_p \cdot e(t) + k_i \int e(t)\,dt + k_d \frac{de(t)}{dt} \tag{16}$$

The proportional term produces an output that is proportional to the current error. It provides an

immediate correction based on the magnitude of the error. The integral term integrates the error over time, addressing any accumulated offset that the proportional term alone cannot correct. It helps eliminate steady-state error. The derivative term responds to the rate of change of the error, providing a damping effect that improves system stability and reduces overshoot [3] [17] [25] [28].

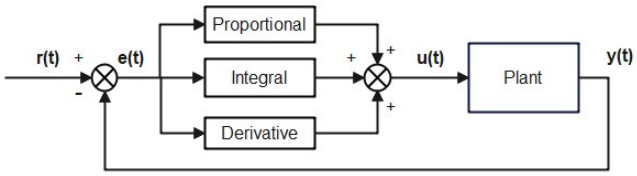

Figure 5. PID Controller

2.5. Fuzzy Logic

Fuzzy logic starts with the concept of a fuzzy set. A fuzzy set is a set without a crisp, clearly defined boundary. It can contain elements with only a partial degree of membership [14] [29] [30]. A fuzzy logic system typically consists of three main steps:

- Fuzzification: Involves converting crisp numerical inputs into fuzzy sets using membership functions.
- Fuzzy Inference: Applies fuzzy rules to determine how inputs map to outputs.
- Defuzzification: Converts fuzzy results back into crisp numerical values

The block diagram of a typical fuzzy logic controller is shown in Figure 6.

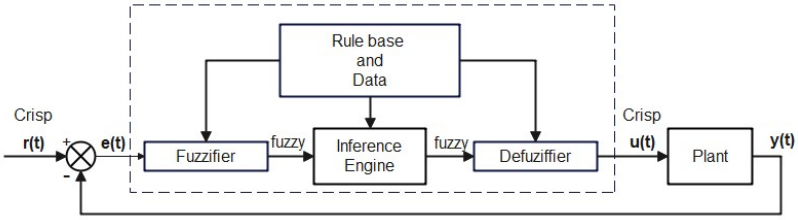

Figure 6. Fuzzy Logic Controller

1) Membership Functions

A membership function is a curve that defines how each point in the input space is mapped to a membership value (or degree of membership) between 0 and 1. The function itself can be an arbitrary curve whose shape we can define as a function that suits us from the point of view of simplicity and efficiency [14] [27] [31]. The simplest membership functions are formed using straight lines. Of these, the simplest is the triangular membership function, and it has the function name trimf. This function is nothing more than a collection of three points forming a triangle as shown in Figure 7.

2) If-Then Rules

If-then rule statements are used to formulate the conditional statements that comprise fuzzy logic. A single fuzzy if-then rule assumes the form If x is A, then y is B where A and B are linguistic values defined by fuzzy sets on the ranges (universes of discourse) X and Y, respectively [14] [29].

3) Fuzzy Inference System

A fuzzy inference system (FIS) is the central unit in a fuzzy logic system, responsible for reasoning and decision making. The main types of FIS are the Mamdani Fuzzy Inference System which uses fuzzy sets and rules to determine outputs and the Sugeno Fuzzy Inference System which uses mathematical functions instead of fuzzy sets [15].

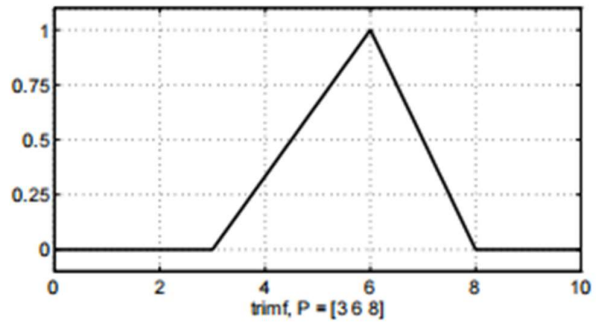

Figure 7. trimf [13]

4) Defuzzification Techniques

Defuzzification is the process of converting fuzzy output values obtained from a Fuzzy Inference System into a single crisp value. Several defuzzification techniques exist, including: The Centroid Method, Weighted Average Method, Bisector Method. Among these, the centroid method is the most commonly used [15] [18] [19].

The Centroid Method (Center of Gravity or Center of Area) calculates the defuzzified output as the center of mass of the fuzzy set.

$$\text{Crisp value} = \frac{\text{Weighted integral of output variable}}{\text{Total area under aggregated membership function}} \quad (17)$$

3. Methodology

3.1. Block Diagram

For speed control of PMSMs, electric vehicles typically employ a FOC scheme which uses Park and Clarke transformations to decouple the torque and flux producing currents. Inverse Clarke and inverse Park transformations convert the dq voltages back to abc voltages for inverter switching.

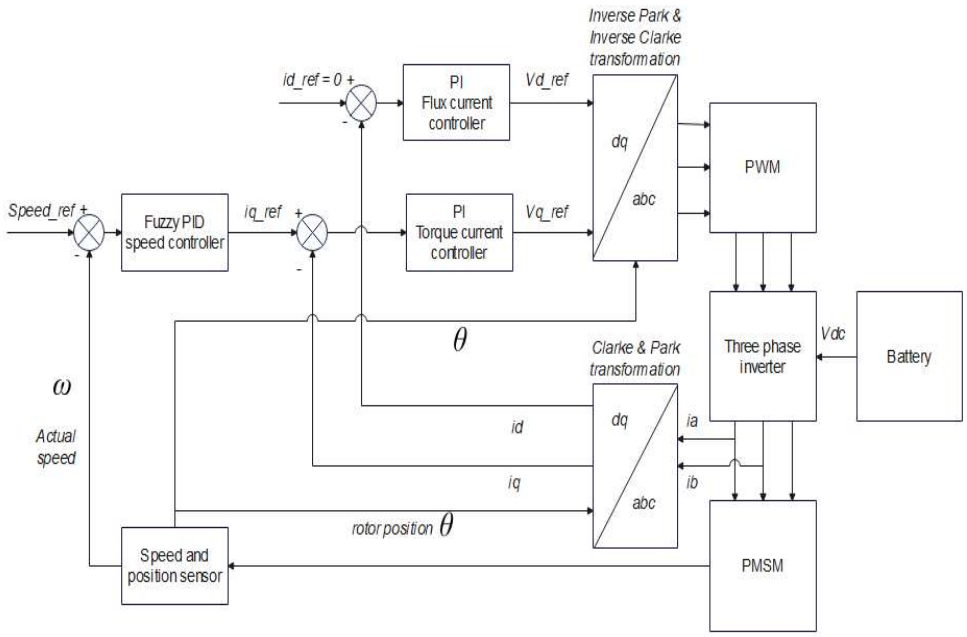

Figure 8. Schematic Diagram of PMSM Field Oriented Control Scheme

Current Controllers

The PI controllers regulate i_d and i_q to achieve flux and torque control. They work in dq frame by generating the control reference voltages v_d and v_q.

$$i_q(s)=\frac{v_q(s)-\omega L_d i_d(s)-\omega\lambda_m}{L_q s+R} \tag{18}$$

Ignoring the cross-coupling terms, the open loop transfer function simplifies to:

$$G(s)=\frac{i(s)}{v(s)}=\frac{1}{Ls+R} \tag{19}$$

This transfer function indicates that the system is a first order system with a gain of $1/L$ and time constant of L/R. The standard PI controller in Laplace domain is,

$$G_{PI}(s)=K_p+\frac{K_i}{s}=K_p\left(1+\frac{1}{T_i s}\right) \tag{20}$$

The open loop transfer function is,

$$G_{OL}(s)=G_{PI}(s)G(s)=K_p\left(1+\frac{1}{T_i s}\right)\left(\frac{1}{Ls+R}\right) \tag{21}$$

The closed loop transfer function is got from,

$$G_{CL}(s)=\frac{G_{OL}(s)}{1+G_{OL}(s)} \tag{22}$$

$$G_{CL}(s)=\frac{i^*}{i}=\frac{K_p\left(1+\frac{1}{T_i s}\right)\left(\frac{1}{Ls+R}\right)}{1+K_p\left(1+\frac{1}{T_i s}\right)\left(\frac{1}{Ls+R}\right)}=\frac{K_p(T_i s+1)}{s^2+\frac{(K_p+R)s}{L}+\frac{K_p}{T_i L}} \tag{23}$$

We compare with the second order closed loop transfer function,

$$\mathrm{T_{CL}}=\frac{\omega_n^2}{s^2+2\zeta\omega_n s+\omega_n^2} \tag{24}$$

Where ζ is the damping ratio and ω_n is the natural frequency,

$$K_p=2\zeta\omega_n L-R \tag{25}$$

$$T_i=\frac{2\zeta\omega_n L-R}{\omega_n^2 L} \tag{26}$$

$$K_i=\omega_n^2 L \tag{27}$$

Direct axis current controller

$$v_d(s)=K_p e_d+\frac{K_i}{s}e_d \tag{28}$$

Where the current error is,

$$e_d=i_d^*-i_d \tag{29}$$

Quadrature Axis Current Controller

$$v_q(s)=K_p e_q+\frac{K_i}{s}e_q \tag{30}$$

Where the current error is,

$$e_q=i_q^*-i_q \tag{31}$$

Speed Controller

The PID controller regulates the rotor speed ω, by generating the i_q reference current i_q^*, which is sent to the inner q axis current control loop.

$$i_q^*=K_p e_\omega+\frac{K_i}{s}e_\omega+sK_d e_\omega \tag{32}$$

Where the speed error is,

$$e_\omega=\omega^*-\omega \tag{33}$$

The output of the PID controller is i_q^*, however i_q is limited physically by the motor's current rating.

$$|i_q^*|\leq i_{max} \tag{34}$$

Where i_{max} is the motor's peak rated current.

Noise filter

A low pass filter is added in series to the derivative path. The speed error passes through the low pass filter to produce a filtered signal to eliminate out the high frequency noise. The standard first order low pass filter is;

$$G_{lp}(s)=\frac{N}{s+N}=\frac{1}{\frac{1}{N}s+1} \tag{35}$$

Where N is the cutoff frequency and it's related to the time constant by $\tau=\frac{1}{N}$

Anti-Windup Mechanism

When the PID controller output reaches a saturation limit, the integrator keeps accumulating error. When the error corrects, the integrator takes time to recover, causing overshoot. Anti-windup prevents this by stopping integration when saturation occurs (clamping) or using a feedback loop with anti-windup gain $K_b$with the difference between the saturated output and the unsaturated controller output (back calculation). Clamping prevents further integration when i_q^* reaches its limit, thus preventing accumulation of integral error. The clamping conditions are; the controller output is saturating and the error is the same sign as the controller output.

Fuzzy logic optimization

The inputs chosen are the speed error and the change of speed error which is the difference between current and previous error. Change in error tells how fast and in which direction the error is.

$$e(t)=\omega_m^*(t)-\omega_m(t) \tag{36}$$

$$ce(t)=e(t)-e(t-1) \tag{37}$$

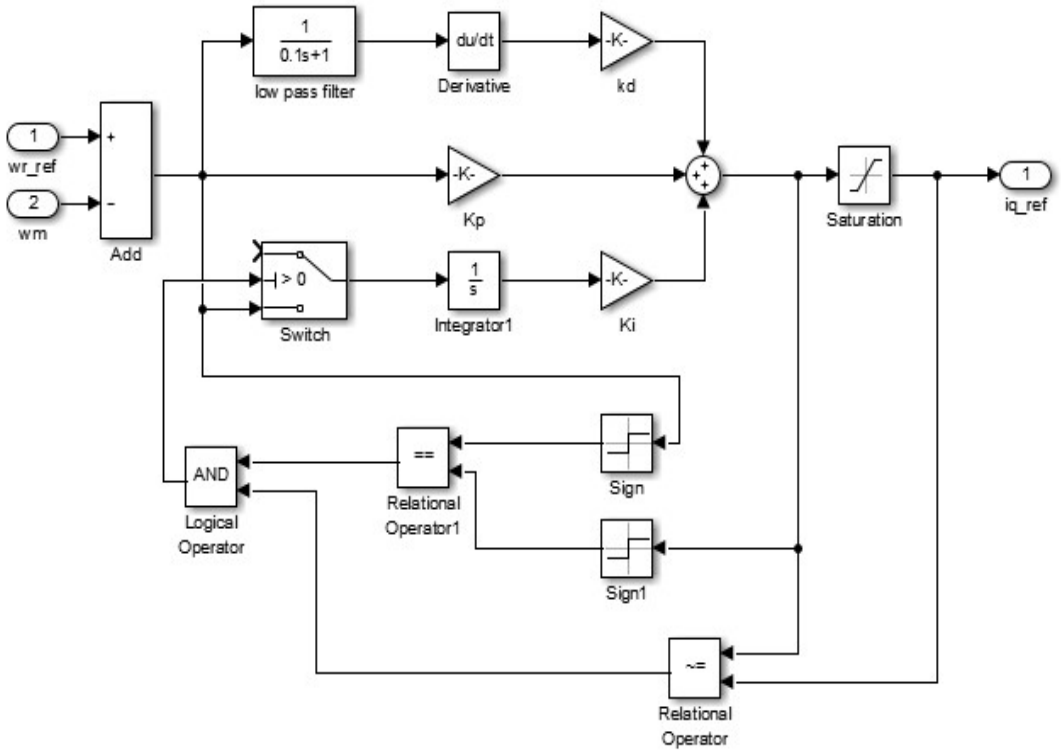

Figure 9. Speed PID Controller Block

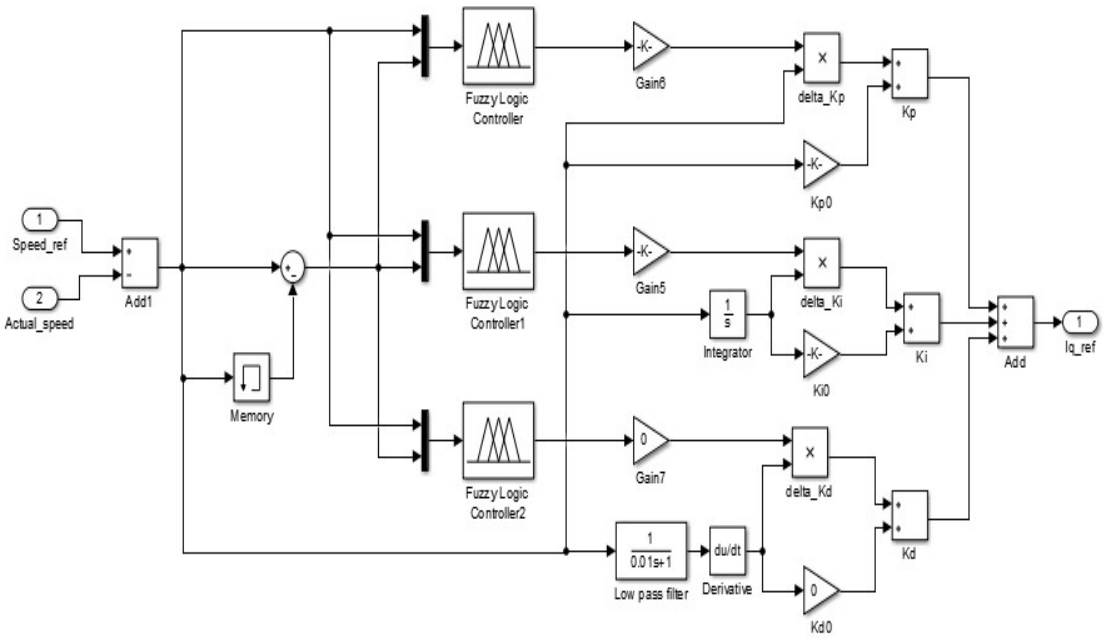

Figure 10: Fuzzy PID Block Model

The linguistic variables for the inputs are Negative large (NL), Negative medium (NM), Negative small (NS), Zero(Z), Positive small (PS), Positive Medium (PM), and Positive large (PL).

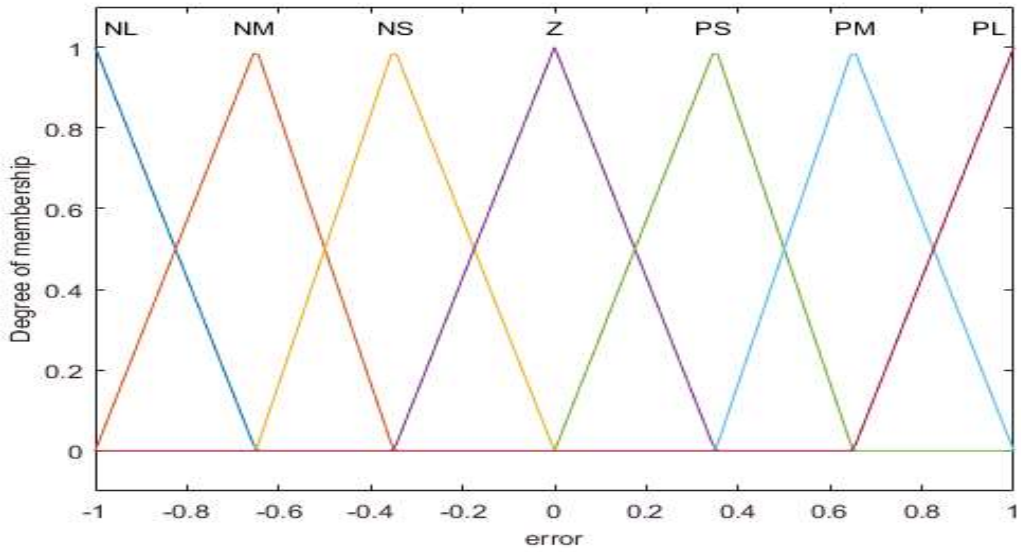

Figure 11. Membership Functions For Speed Error Input

The linguistic variables for outputs are Very small (VS), Medium small (MS), Small (S), Medium (M), Large (L), Medium Large (ML), and Very Large (VL). This gives 49 rules.

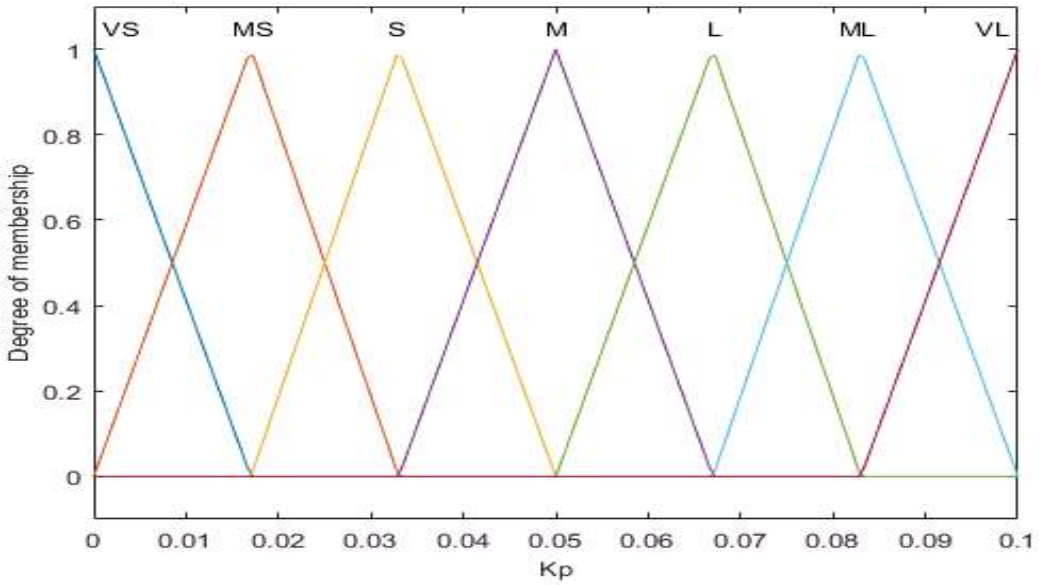

Figure 12. Membership Functions for the Kp Output

The rule base is chosen from an understanding of the PID gains and their effects on system response. If the speed error is large, increase k_p aggressively to reduce rise time. If error is near zero, keep k_p

moderate to avoid overshoot and If error is decreasing fast, reduce k_p to prevent overshoot. For the k_i output, if error is large, keep k_i moderate to avoid windup. If error is small but persistent, increase k_i to eliminate steady-state error. If error is decreasing, reduce k_i to prevent overshoot. For k_d, if error is near zero, keep k_d moderate to avoid excessive damping. If error is changing rapidly, adjust k_d aggressively to improve stability.

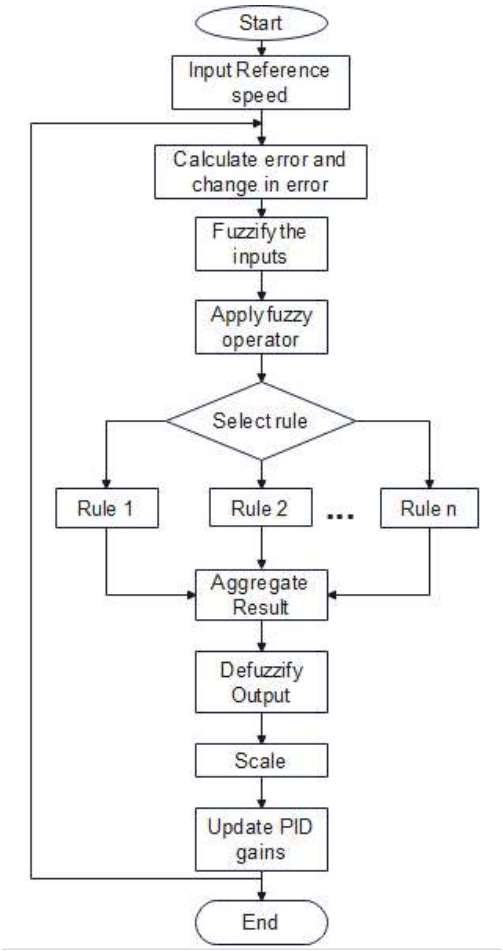

Figure 13. Fuzzy Reasoning Flowchart

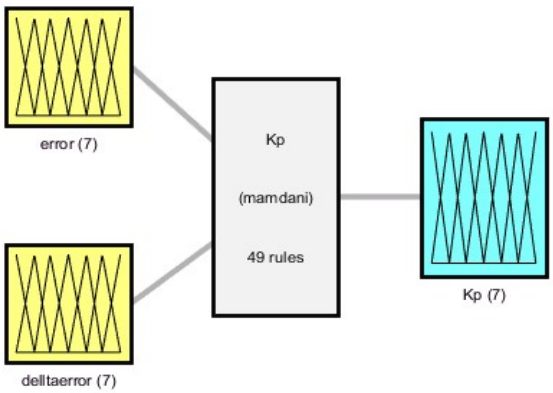

Figure 14. k_p fuzzy Inference System

Table 1. Rule Base for Δk_p

e | ce	NL	NM	NS	Z	PS	PM	PL
NL	VL	VL	VL	VL	ML	L	M
NM	VL	VL	VL	ML	L	M	S
NS	VL	VL	ML	L	M	S	MS
Z	VL	ML	L	M	S	MS	VS
PS	ML	L	M	S	MS	VS	VS
PM	L	M	S	MS	VS	VS	VS
PL	M	S	MS	VS	VS	VS	VS

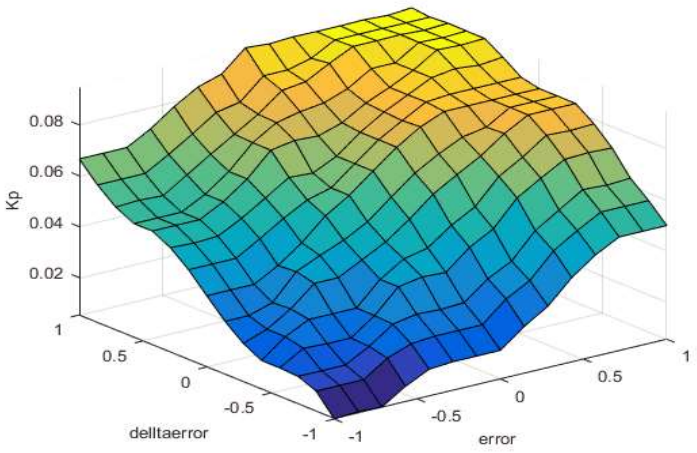

Figure 15. Control Surface for k_p

4. Finding and Discussion

4.1. Paramaters

Motor parameters shows in Table 2.

Table 2. Motor Parameters

Parameter	Symbol	Value	Units
Poles	P	4	-
Stator winding resistance	R	18.7	Ω
Inductance	L_d,L_q	0.02682	H
Permanent magnet flux	λ_m	0.18	Wb
Rotor inertia constant	J	0.0008	Kgm^2
Damping constant	B	0.00001	Kg/s

Table 3. Controller Gain Values

Controllers	Speed Controller gains			Current controller gains			
				D axis		Q axis	
	Kp	Ki	Kd	Kp	Ki	Kp	Ki
PID	0.014	0.19	0.0001	71.54	$1.52e^5$	71.54	$1.52e^5$
Fuzzy PID	Updated each sampling			71.54	$1.52e^5$	71.54	$1.52e^5$

4.2. FOC Model

The simulation environment is MATLAB/Simulink 2016, PWM frequency is 20kHz, sampling time is $1e^{-6}$s and a simulation time of 2 seconds.

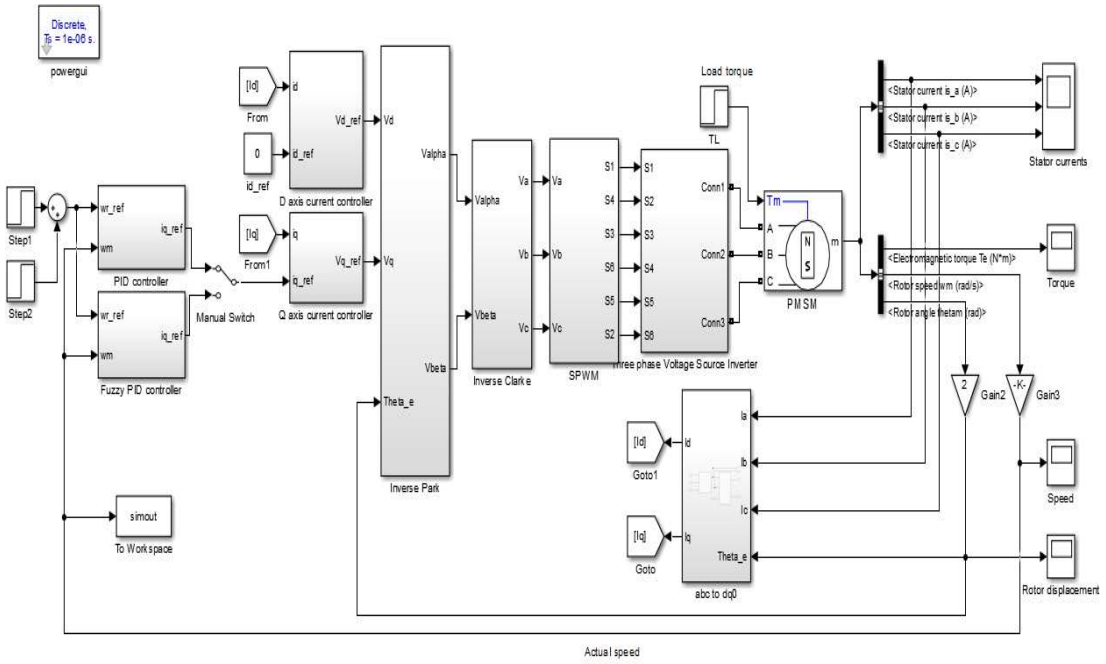

Figure 16. Complete Field Oriented Control Scheme

1) No Load Test

A reference speed of 500 rpm is set and no-load torque is put on the machine.

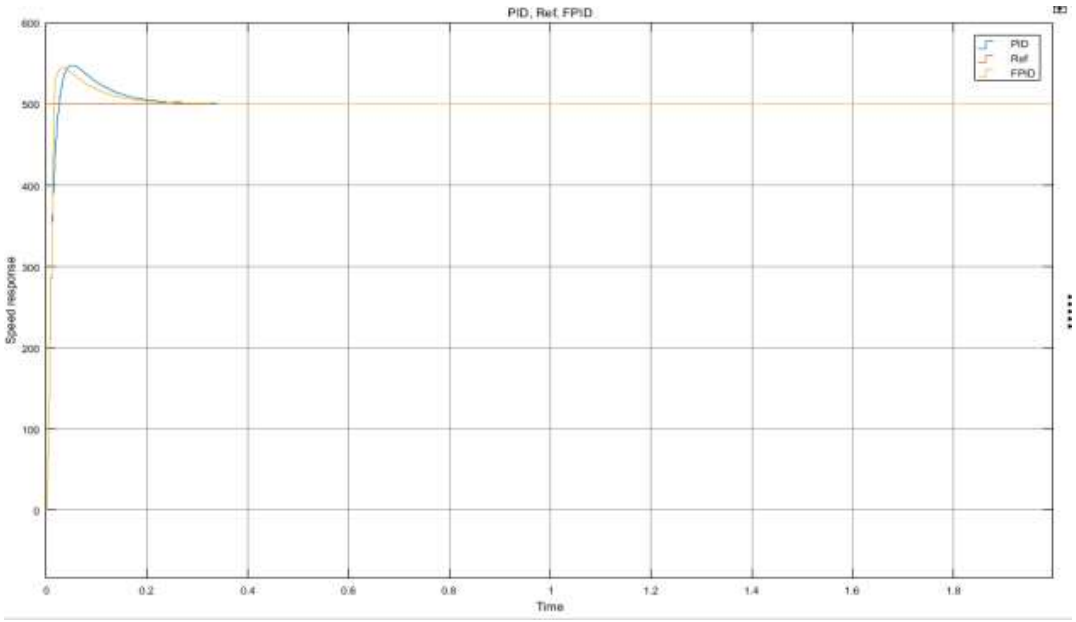

Figure 17. Speed Response at No Load

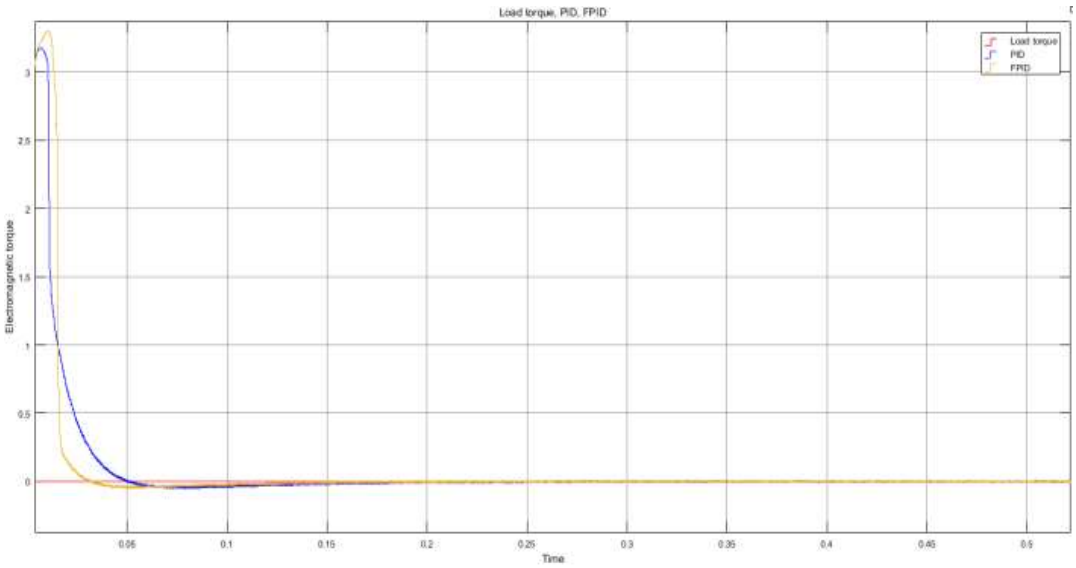

Figure 18. Torque Response at No Load

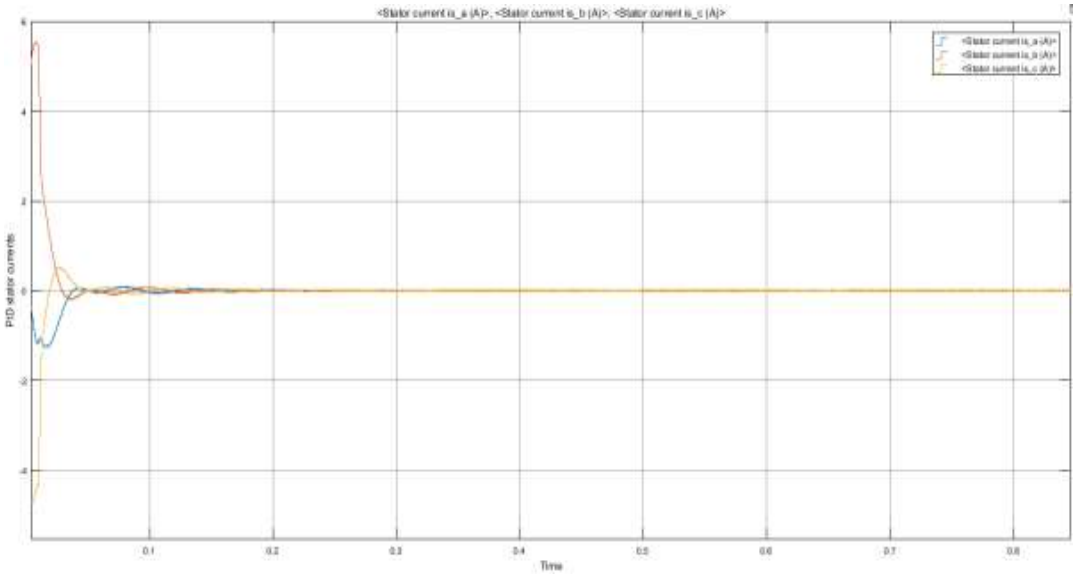

Figure 19. Stator Currents at No Load

Both controllers experience some overshoot, however the fuzzy PID controller achieves less overshoot of 8.3% to the PID's 9.34%. The fuzzy PID also achieves a faster rise time of 10.421ms and the PID, 15.362ms as shown in Figure 17. The PMSM has a high starting torque but since no load has been placed on the motor, the electromagnetic torque reduces to approximately zero to support only the retard friction as shown in Figure 18. The electromagnetic torque affects the amplitude of the stator currents. Initially at high starting torque, the stator currents have a large amplitude but quickly approximate to zero at steady state because no load has been placed on the motor as shown in Figure 19.

2) Constant Load Test

A constant load of 1Nm is placed on the motor and two incremental speeds are subjected to the motor at t = 0s and t = 0.65s of 200rpm and 300rpm respectively before breaking at t = 1.4s.

Journal of Engineering, Technology & Applied Science, vol. 7, no. 3, pp. 127-148, December 2025. **DOI: 10.36079/lamintang.jetas-0703.917**

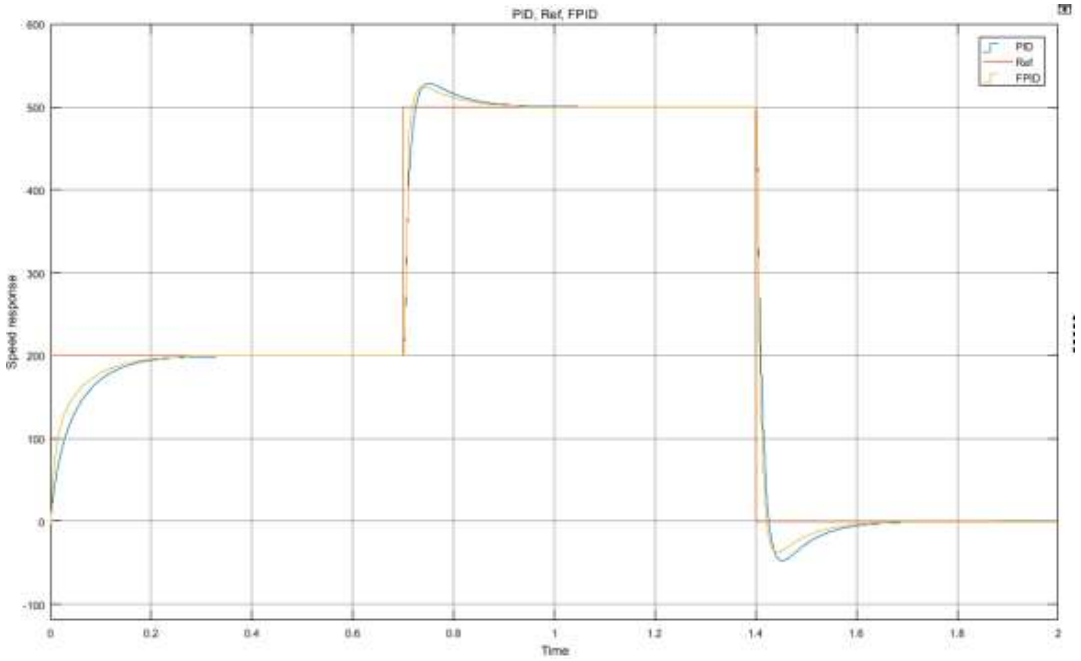

Figure 20. Speed Response at Varying Loads

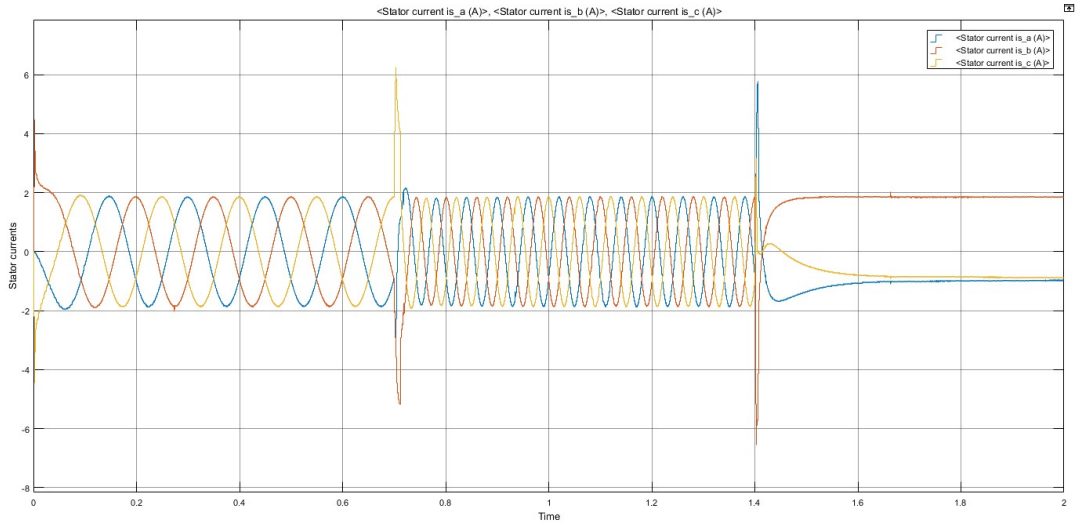

Figure 21. Stator Currents For Speed Variation at a Constant Load

The fuzzy PID outperforms the PID controller with a faster rise time of 10ms, less overshoot of 8.4%. The PID experiences a rise time of 16.6ms, overshoot of 8.9%. The stator currents have the same amplitude after each change but have different frequencies as shown in Figure 20. This is because reference speed input affects the stator currents frequency, when the reference speed is increased, the stator currents frequency also increases and vice versa. The amplitude spikes of the currents are due to the transient torque variations. This is because of the cross coupling between the torque and flux components of the dq currents.

3) Load Variation Test

A constant speed of 500rpm is applied. An initial load torque of 0.5Nm is put on the motor, then at t = 0.63s another load of 0.5Nm is added, finally at t = 1.4s a load of 0.7Nm is removed from the motor.

Journal of Engineering, Technology & Applied Science, vol. 7, no. 3, pp. 127-148, December 2025. **DOI: 10.36079/lamintang.jetas-0703.917**

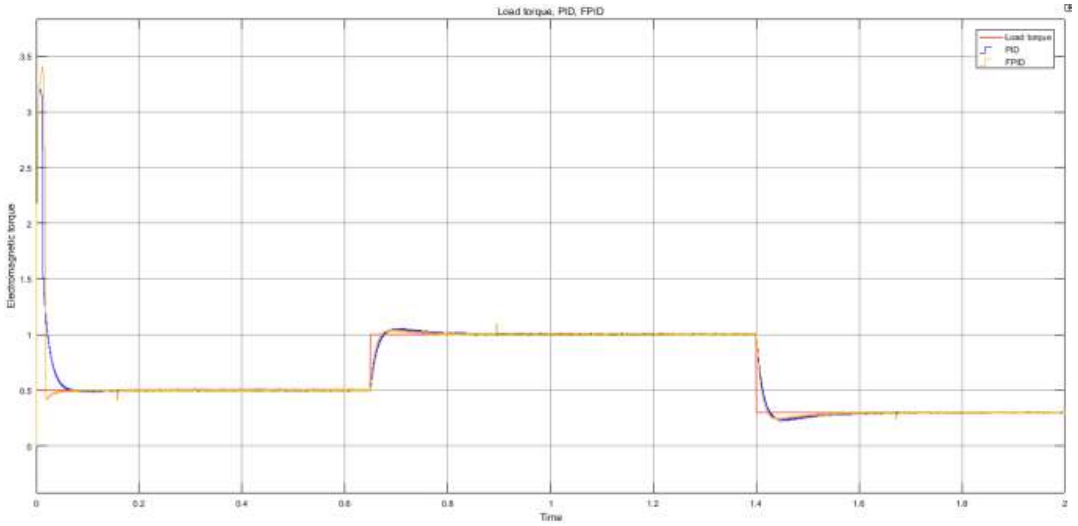

Figure 221. Electromagnetic Torque at Varying Loads

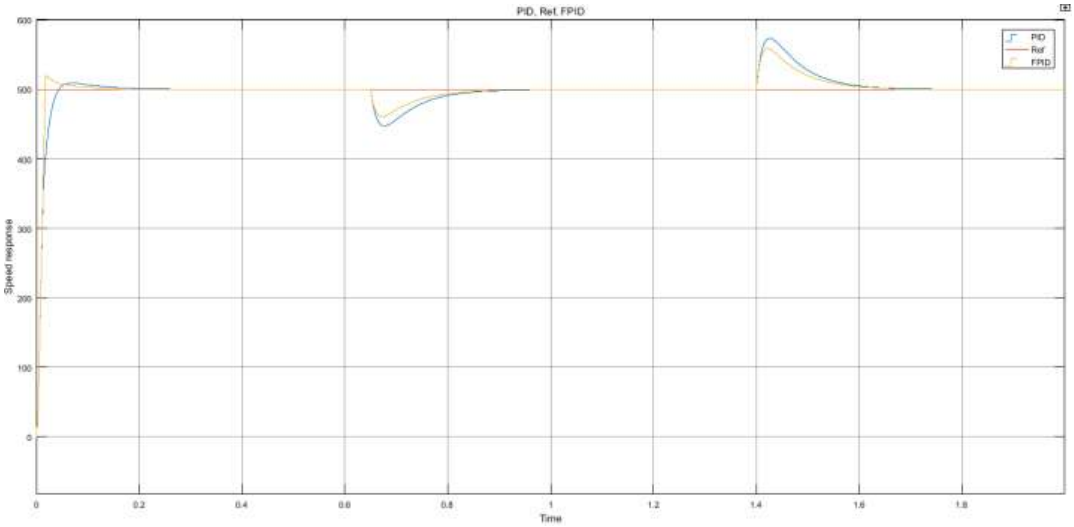

Figure 232. Speed Response at Varying Loads

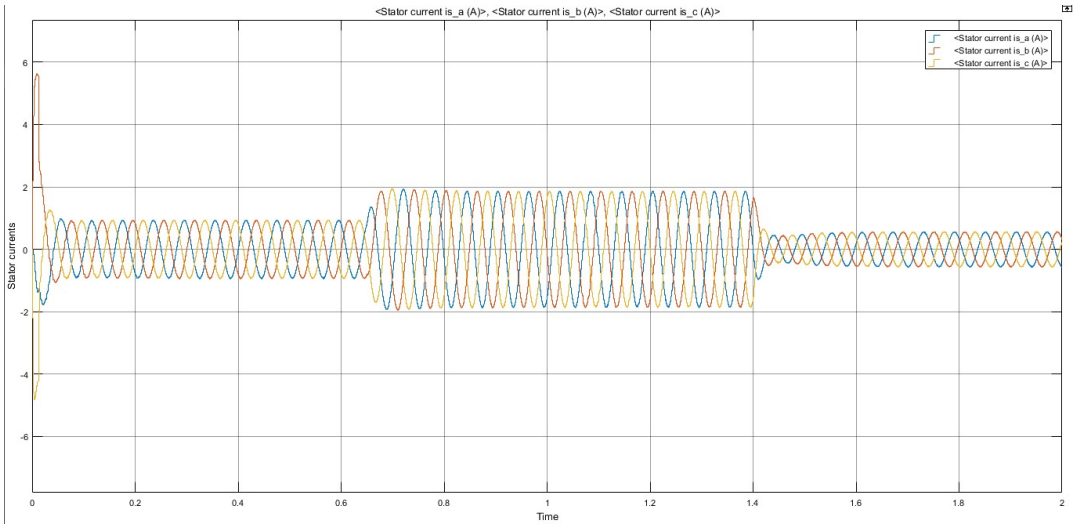

Figure 243. Stator Currents at Varying Loads

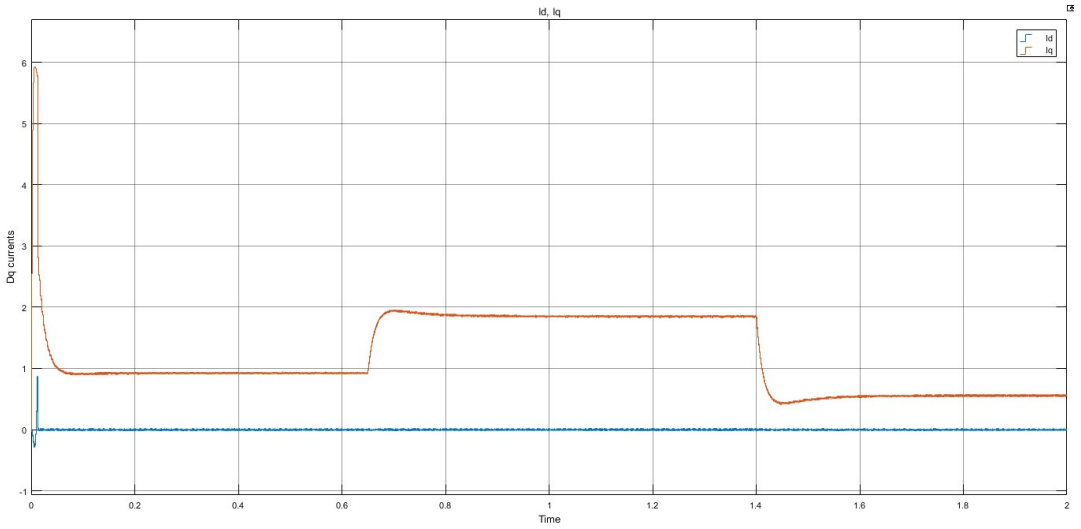

Figure 25. Dq Currents at Varying Loads

Initially the electromagnetic torque is high because of the high starting torque of the motor but it quickly achieves a steady state of 0.5Nm and then varies with the set load torques as shown in Figure 21. The fuzzy PID controller achieves a faster rise time of 12.07ms but it however produces more overshoot initially which is undesirable. The PID controller achieves a rise time of 21.58ms. The stator currents amplitudes vary with the load torques; stator currents amplitude increases at t = 0.63s when the load torque is increased to 1Nm but they decrease when a load torque of 0.7Nm is removed from the motor as shown in Figure 24. As expected, the i_d current component is fairly constant but the i_q current component varies with the load torque applied on the motor as shown in Figure 25.

Another simulation of Stator currents and electromagnetic torque at increasing loads from 0Nm at t = 0s, 0.5Nm increments at t = 0.5s, t = 1s and t = 1.5s.

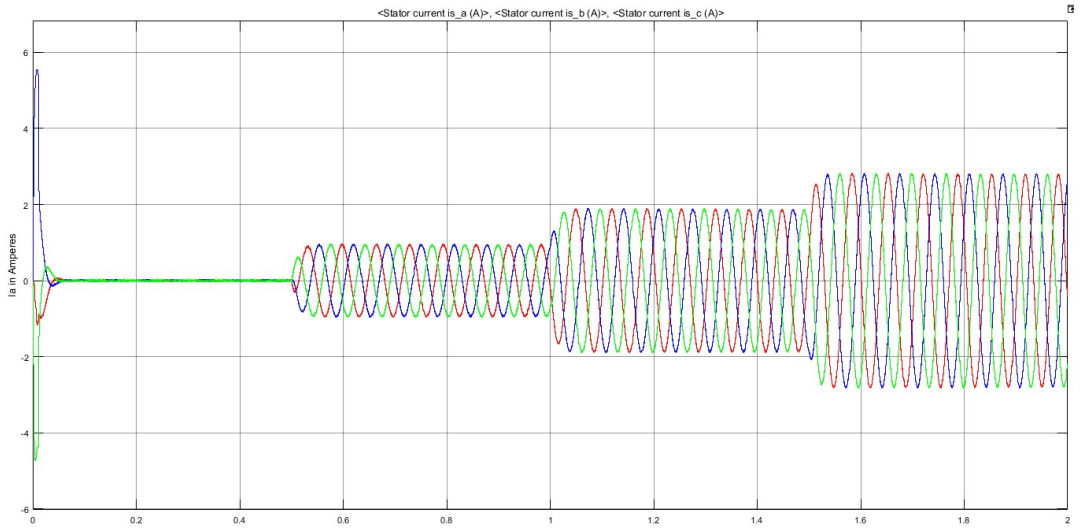

Figure 26. Stator Currents at Increasing Loads

As expected, we get increasing amplitudes for the stator currents but their frequency remains the same as shown in Figure 26. This is because the speed applied is constant. The electromagnetic torque varies with the load torque increments as shown in Figure 27.

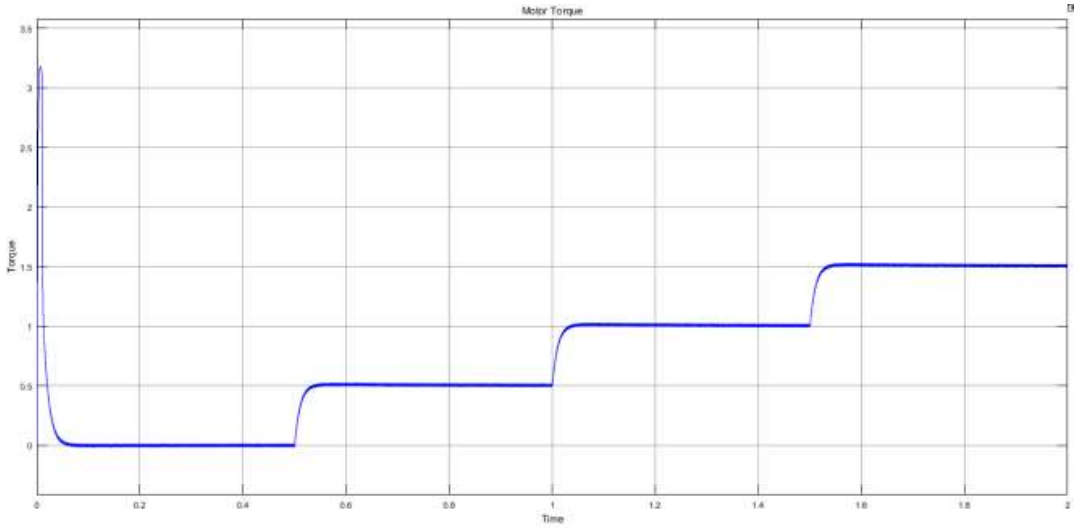

Figure 27. Electromagnetic Torque at Increasing Loads

4) Parameter Variation

Motors heat up during prolonged operation, this affects the stator resistance, inductance and permanent magnet flux which vary with increase in motor temperature. Considering the temperature dependence of the copper windings in the stator. The stator resistance is given by,

$$R_t = R_0(1+\alpha\Delta T) \tag{39}$$

where by R_0 is the resistance of the copper windings at standard temperature (25℃),

α is the temperature coefficient of copper ($0.00393℃^{-1}$)
ΔT is the change in temperature.

Assuming a temperature above the normal operating temperature of 100℃, the stator resistance becomes 24.2Ω.

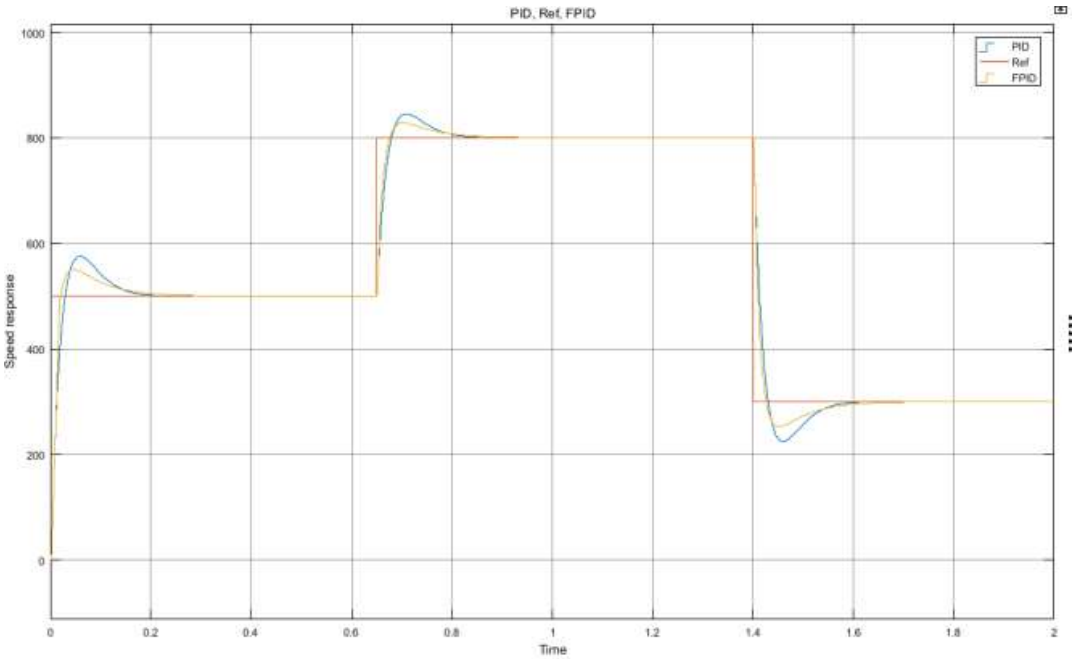

Figure 28. Speed Response at 24.2Ω Stator Resistance

Both controllers track the reference speed, however the fuzzy PID controller achieves a better performance of 653ms rise time, 5.83% overshoot. The PID gets 655.36ms rise time, 9.32% overshoot. The fuzzy PID controller tunes the PID gains dynamically to minimise overshoot and reduce the rise time even when the parameters of the machine vary.

Table 4. Summary of Results

	Rise time		**Settling time**		**Overshoot**	
	PID	**FPID**	**PID**	**FPID**	**PID**	**FPID**
No load test	15.36ms	10.42ms	19.879ms	18.28ms	8.3%	9.34%
Constant load test	16.6ms	10ms	17.04ms	---	8.9%	8.4%
Load variation test	21.58ms	12.07ms	---	---	2.3% undershoot	1.9% undershoot
Parameter variation test	35.36ms	23ms	---	---	9.32%	5.83%

5. Conclusion

This paper addresses the limitations of conventional PID controllers in the speed control of Permanent Magnet Synchronous Motors used in electric vehicle propulsion systems. Through detailed modeling and simulation in MATLAB/Simulink, the study successfully demonstrates that the Fuzzy PID controller significantly outperforms the conventional PID controller across a range of performance metrics. Notably, it achieved faster settling times, reduced overshoot, and improved speed tracking under both constant and varying load conditions. A compelling case for the adoption of intelligent hybrid control systems in electric vehicle propulsion.

This paper focuses on software simulation, future research should consider hardware in the loop simulation or real time embedded implementation using digital signal processors to validate the controller's effectiveness in practical settings. Additionally, integrating advanced optimization techniques like Genetic Algorithms, Neural networks or Reinforcement Learning with fuzzy control may yield even more efficient tuning and thus better results. Lastly, the designed controller could be combined with a simulation of the wider EV drive train to fully assess its impact on the mechanical components of the vehicle thus giving a well-rounded view of ride comfort.

References

[1] W. Xu, M. M. Ismail, and M. R. Islam, *Permanent Magnet Synchronous Machines and Drives: Flux Weakening Advanced Control Techniques*. CRC Press, 2023.

[2] H. O. Erkol, "Optimized Field Oriented Control Design by Multi Objective Optimization," *International Journal of Advanced Computer Science and Applications*, 2019.

[3] A. Visioli, "Pid control system design and automatic tuning using matlab/simulink," *IEEE Control Systems Magazine*, vol. 41, no. 3, pp. 99-100, 2021.

[4] J. G. Ziegler and N. B. Nichols, "Optimum settings for automatic controllers," *ASME Journal of Dynamic Systems, Measurement, and Control*, vol. 115, no. 2B, pp. 220-222, 1993.

[5] R. P. Borase, D. K. Maghade, S. Y. Sondkar, and S. N. Pawar, "A review of PID control, tuning methods and applications," *International Journal of Dynamics and Control*, vol. 9, no. 2, pp. 818-827, 2021.

[6] I. Voncila, I. Paraschiv, and M. Costin, "The Influence of Saturation on the Performance of PMSM," in *7th International Symposium on Electrical and Electronics Engineering*, Galati, Romania, 2021, pp. 1-6.

[7] O. E. Özçiflikçi, M. Koç, S. Bahçeci, and S. Emiroğlu, "Overview of PMSM control strategies in electric vehicles: A review," *Int. J. Dyn. Control*, vol. 12, pp. 2093–2107, 2024.

[8] F. Amin, E. Sulaiman, and H. Soomro, "Field oriented control principles for synchronous motor," *International Journal of Mechanical Engineering and Robotics Research*, vol. 8, pp. 284-288, 2019.

[9] P. Mohindru, "Review on PID, fuzzy and hybrid fuzzy PID controllers for controlling non-linear dynamic behaviour of chemical plants," *Artificial Intelligence Review*, vol. 57, no. 4, p. 97, 2024.

[10] I. Voncila, I. Paraschiv, and M. Costin, "The Influence of Saturation on the Performance of PMSM," in *7th International Symposium on Electrical and Electronics Engineering*, Galati, Romania, 2021, pp. 1-6.

[11] H. Chen, W. Liu, and Y. Li, "Comprehensive Design and Analysis of an Interior Permanent Magnet Synchronous Machine for Light Duty Passenger EVs," *IEEE Transactions on Transportation Electrification*, vol. 7, no. 1, pp. 123-134, 2021.

[12] E. Hernández-Mayoral et al., "A comprehensive review on power-quality issues, optimization techniques, and control strategies of microgrid based on renewable energy sources," *Sustainability*, vol. 15, no. 12, p. 9847, 2023.

[13] M. A. Azom and M. Y. A. Khan, "Recent developments in control and simulation of permanent magnet synchronous motor systems," *Control Systems and Optimization Letters*, vol. 3, no. 1, pp. 84-91, 2025.

[14] R. Jang and N. Gulley, *Fuzzy Logic Toolbox™ User's Guide, MATLAB R2021b*. The MathWorks, Inc., 2021.

[15] G. Filo, "A review of fuzzy logic method development in hydraulic and pneumatic systems," *Energies*, vol. 16, no. 22, p. 7584, 2023.

[16] I. M. Cabral, J. S. Pereira, and J. B. Ribeiro, "Performance evaluation of PID and Fuzzy Logic controllers for residential ORC-based cogeneration systems," *Energy Conversion and Management: X*, vol. 23, p. 100622, 2024.

[17] W. Ahmed, M. Adel, M. Taha, and A. Saleh, "PSO technique applied to sensorless field-oriented control PMSM drive with discretized RL-fractional integral," *Alexandria Engineering Journal*, vol. 60, pp. 4029-4040, 2021.

[18] P. V. Chakaravarthi and P. Karpagavalli, "Speed control of PMSM motor using fuzzy and PID controller," *Journal of Selected Areas in Microelectronics*, vol. 8, no. 2, pp. 121-128, 2016.

[19] N. P. Ananthamoorthy and B. K. Baskaran, "High performance hybrid fuzzy PID controller for permanent magnet synchronous motor drive with minimum rule base," *Journal of Vibration and Control*, vol. 21, no. 1, pp. 181-194, 2015.

[20] S. Gupta, S. George, and V. Awate, "PI Controller Design and Application for SVPWM Switching Technique Based of PMSM," in *Second International Conference on Trends in Electrical, Electronics and Computer Engineering*, Bangalore, India, 2023, pp. 172-177.

[21] A. Sergakis, M. Salinas, N. Gkiolekas, and K. N. Gyftakis, "A Review of Condition Monitoring of Permanent Magnet Synchronous Machines: Techniques, Challenges and Future Directions," *Energies*, vol. 18, no. 5, p. 1177, 2025.

[22] R. P. Borase *et al.*, "A review of PID control, tuning methods and applications," *International Journal of Dynamics and Control*, vol. 9, pp. 818-827, 2021.

[23] F. Jin, H. Wan, Z. Huang, and M. Gu, "PMSM Vector Control Based on Fuzzy PID Controller," *Journal of Physics: Conference Series*, vol. 1617, 2020.

[24] A. Benevieri et al., "'Surface Permanent Magnet Synchronous Motors' Passive Sensor less Control: A Review," *Energies*, vol. 15, no. 57, 2022.

[25] Ł. Lemieszewski and P. Puzio, "Optimization of PID Controller Settings Using the Ziegler–Nichols Method in Pneumatic Pressure Control Systems," *Procedia Computer Science*, vol. 270, pp. 5177-5186, 2025.

[26] Y. Sato, T. Kubota, and A. Chiba, "Research on the Performances and Parameters of Interior PMSM Used for Electric Vehicles," *IEEE Transactions on Magnetics*, vol. 51, no. 11, pp. 1-4, 2015.

[27] A. G. Gad, "Particle swarm optimization algorithm and its applications: A systematic review," *Archives of Computational Methods in Engineering*, vol. 29, no. 5, 2022.

[28] A. Lambora, K. Gupta, and K. Chopra, "Genetic algorithm-A literature review," in *International Conference on Machine Learning, Big Data, Cloud and Parallel Computing*, 2019, pp. 380-386.

[29] A. Balashanmugham and M. Maheswaran, "Permanent Magnet Synchronous Machine Drives," in *Applied Electromechanical Devices and Machines for Electric Mobility Solutions*, IntechOpen, Mar. 25, 2020.

[30] R. Martinek et al., "Design of a Measuring System for Electricity Quality Monitoring within the SMART Street Lighting Test Polygon: Pilot Study on Adaptive Current Control Strategy for Three Phase Shunt Active Power Filters," *Sensors*, vol. 20, 2020.

[31] N. S. Nise, *Control Systems Engineering*. Hoboken, NJ, USA: John Wiley & Sons, 2020.